Pergamon

*Int. J. Heat Mass Transfer.* Vol. 40, No. 13, pp. 3189–3200, 1997

Printed in Great Britain
0017–9310/97 $17.00+0.00

PII: S0017–9310(96)00366–3

# Latent cold heat energy storage characteristics by means of direct-contact-freezing between oil droplets and cold water solution

HIDEO INABA and KENJI SATO

Department of Mechanical Engineering, Faculty of Engineering, Okayama University, Tsushima-naka 3-1-1, Okayama 700, Japan

(*Received* 14 *March* 1996 *and in final form* 18 *September* 1996)

**Abstract**—Flow and solidification characteristics of paraffin oil droplets (tetradecane with the melting point of 5.8°C, the latent heat of fusion of 229.1 kJ/kg and the density of 770 kg/m$^3$ at 6°C) ascending in a cold water solution are experimentally investigated. The tetradecane oil is injected from a cylindrical single hole nozzle into the cold water solution and it disperses and forms tiny oil droplets. The oil droplets ascend in the water solution by buoyancy and freeze by direct-contact heat exchange with the cold water solution. Finally, they are completely or partially frozen. The partially frozen oil droplet is composed of a frozen outer shell and unfrozen central core. As a result, it was found that the solidification fraction of the frozen oil droplets, defined as mass ratio of the solidified parts to the whole, increases with a decrease in injection oil temperature and water solution temperature. However, under a lower temperature condition, the injected oil freezes at the outlet of the nozzle, and the solidification fraction reduces with a decrease in injection oil temperature and water solution temperature. A method of data reduction for the solidification fraction is proposed and non-dimensional empirical equations to predict the solidification fraction are proposed in this study. © 1997 Elsevier Science Ltd.

## INTRODUCTION

In recent years, a large difference between an electric power demand in the daytime and in the nighttime is one of most important issues for energy saving, which occurs due to excessive use of air conditioners during daytime, especially in summer. In order to overcome this problem, studies of latent-heat cold energy storage systems using cheaper electric power at night have been carried out. The latent-heat cold energy storage systems can store a large amount of cold energy in a relatively small heat storage vessel by using phase change material (PCM). Furthermore, outlet temperature of a heat exchange fluid through a heat storage vessel can be almost constant and be almost the same as the melting point of the PCM. Therefore, a desired outlet temperature of the heat exchange fluid can be obtained by a proper selection of PCM. Typical PCM will be ice or paraffin. Latent-heat cold energy storage systems for air conditioning use mainly ice because of its low melting point of 0°C and low cost. The systems using a paraffin wax can apply wide temperature range because we can choose various melting points by changing its component. Coefficient of operation performance (COP) of a refrigerator in a latent-heat cold energy storage system increases with an increase in the melting point of PCM. Therefore, an appropriate paraffin PCM, whose melting point is higher than that of ice, has been desired instead of ice. Another important point in a latent-heat cold energy storage system is of heat transfer during freezing of PCM. In a capsule type heat exchanger often used, PCM is packed in a number of capsules immersed in a heat exchange fluid. The heat is transferred from the heat exchange fluid to PCM through the capsule wall. Therefore, the capsule type heat exchanger has some demerits that it takes longer to complete latent-heat energy storage and the size of the heat energy storage vessel becomes larger, since the capsule wall acts as a thermal resistance. A direct-contact heat exchanger can overcome these problems. Some studies on the direct-contact heat exchanger for a latent-heat cold energy storage are reported [1].

The present study proposes a new kind of latent cold heat energy storage system using a tetradecane as PCM instead of ice and using a spray-tower type direct-contact heat exchange composed of PCM oil droplets and a heat exchanger fluid. As indicated in Table 1 [2], tetradecane has a higher melting point of 5.8°C compared with that of ice, however, it is still appropriate for air conditioning. Therefore, a higher value of COP is expected. In the heat exchanger dealt with in this study, the PCM oil droplets behave as a dispersed phase and the cold heat transfer fluid behaves as a continuous phase.

A large number of excellent literatures about spray tower heat exchangers have been seen today, which concern heat and mass transfer characteristics between dispersed and continuous phases [3–6]. In addition, the studies on the dispersion of a liquid jet injected into immiscible liquid and the drop formation characteristics [7–9] and the correlation between

## NOMENCLATURE

$c_{ds}$ specific heat of solid phase tetradecane
$d_n$ nozzle diameter
$d_p$ diameter of dispersed phase droplet
$\bar{d}_p$ arithmetic mean diameter of dispersed phase droplet
$F$ cross-sectional area of the group of ascending dispersed phase droplets
$h_1$, $h_2$ liquid levels in the glass tube of the volumeter
$\Delta h$, $\Delta h_0$ liquid level displacements in the glass tube of the volumeter
$L$ latent heat of tetradecane
$m_t$, $m_{tf}$ mass of sampled frozen oil droplet
$N$ the number of dispersed phase droplets in a test volume for visualization
$R$ solidification of frozen oil droplets
$R^*$ modified solidification fraction
$Re_{pc}$ characteristic Reynolds number of dispersed phase droplets
$Ste$ Stefan number
$T_c$ temperature of water solution
$T_m$ melting point of tetradecane (= 5.8°C)
$T_n$ injection temperature of tetradecane oil
$U_c$ velocity of water solution in the test section
$U_p$ ascending velocity of formed droplets
$U_{pc}$ characteristic ascending velocity of the formed droplets
$U_n$ injection velocity of the tetradecane oil ($= V_d/[\pi(d_n/2)^2]$)
$V_d$ volumetric flow rate of the tetradecane oil
$x$ modified non-dimensional temperature ratio
$Y$ vertical distance from the nozzle outlet to droplet
$Y_0$ vertical distance from the nozzle outlet to the top surface of the water solution
$\Delta Y$ height of test volume for visualization.

Greek symbols
$\varepsilon$ volumetric packing ratio of formed droplets
$\theta$ nondimensional temperature ratio
$\nu_c$ kinematic viscosity of water solution.

Subscripts
c water solution
d tetradecane oil
n nozzle, injection
p dispersed phase droplet.

Table 1. Physical properties of tetradecane [2]

| | | |
|---|---|---|
| Melting point (°C): 5.8 | | |
| Latent heat (kJ/kg): 229.1 | | |
| | (Liq. (6°C)) | (Sol. (5°C)) |
| Specific heat (kJ/kgK): | 2.0 | 1.8 |
| Density (kg/m$^3$): | 770 | 810 |

diameter and velocity of a drop rising or falling in a continuous phase [10, 11] are available for spray tower heat exchanger. Some studies on direct-contact heat exchange with a phase-change have been carried out mainly about a direct-contact evaporation and condensation [12–14]. However, there have been fewer studies about direct-contact heat exchange in which a liquid drop of the dispersed phase causes solidification [15, 16]. For example, in the previous works, there have been theoretical studies on solidification of a drop, a plane or spherical thin melted film [17–19]. Especially, Petrescu and Fetecau [20] performed a theoretical study on a temperature profile and a cooling duration of a drop falling freely in a fluid. Some experimental studies have been also seen about peal granulation in a liquid or gaseous media [21, 22].

The previous researches have studied fundamental heat transfer characteristics between formed droplet and continuous phase liquid under a certain condition. However, the target of the present study is to investigate the overall performance of a direct-contact type heat exchanger in which the formed droplets freeze, with a view to apply this phenomenon to latent cold energy storage systems. A few studies have been conducted in this field [23, 24]. In this paper, the dispersion of PCM liquid and the solidification of PCM droplets in a heat exchange fluid with a low temperature are experimentally investigated.

## EXPERIMENTAL APPARATUS AND PROCEDURE

Tetradecane and ethylene glycol water solution of 30 mass percent are used as PCM and a heat exchange fluid, respectively. Physical properties of both materials are indicated in Table 1 [2]. As shown in Fig. 1, an experimental apparatus consists mainly of a cold water solution circulating loop, tetradecane oil injection system and a test section. The temperature of the water solution is controlled by a constant temperature bath (2) (a minimum controllable temperature is 0.1°C) and it flows into the upper part of the test section (4) through an overflow tank (1). The

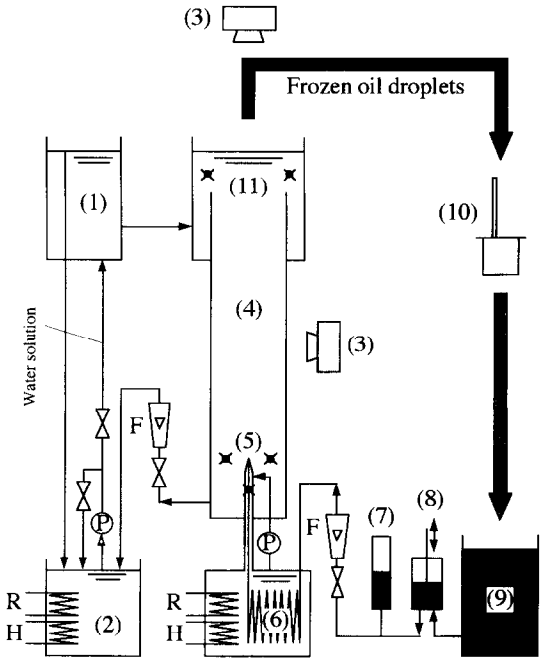


(1) Overflow tank
(2) Constant temperature bath
(3) Camera
(4) Test section
(5) Nozzle
(6) Tetradecane temperature regulator
(7) Pressure pulse damping tank
(8) Diaphragm pump
(9) Tetradecane oil tank
(10) Volumeter
(11) Reservoir tank
H Heater
R Refrigerator
F Flow-meter
Thermocouple

Fig. 1. Schematic diagram of experimental apparatus.

water solution flows downward in the test section with very slow velocity ($U_c = -7.0 \times 10^{-3}$ m/s) and it returns to a constant temperature bath after passing through a flow rate control valve and a float-type flow-meter (the measuring range is $0.5 \sim 5.0 \times 10^{-6}$ $m^3/s$, the measuring precision is $9.0 \times 10^{-8}$ $m^3/s$). The tetradecane oil is pressed out from an oil tank (9) by a diaphragm pump (8) (the maximum flow rate is $4.0 \times 10^{-6}$ $m^3/s$, the maximum head is 392 kPa). It passes through a pressure pulse damping tank (7), two float-type flow-meters (the one has the measuring range of $0.167–1.67 \times 10^{-6}$ m3/s and the measuring precision of $3.0 \times 10^{-8}$ $m^3/s$, the other has the measuring range of $0.2–2.0 \times 10^{-7}$ $m^3/s$ and the measuring precision of $3.5 \times 10^{-9}$ $m^3/s$), a needle valve for controlling flow rate, temperature regulator (6) (the minimum controllable temperature is 0.1°C). A double pipe is used between the nozzle and a temperature regulator (6). The tetradecane oil flowing in the inner pipe of a double pipe is thermally insulated by a high temperature brine, flowing in an outer clearance in the double pipe, which is extracted from a temperature regulator (6). The tetradecane oil injected from the nozzle splits into many tiny oil droplets (see Fig. 2). The oil droplets ascend in the water solution by buoyancy. During ascending, the oil droplets start to solidify by a direct-contact cooling with the cold water solution surrounding them. The solidification progresses from the surface of the oil droplets toward the center of them. When they arrive at the top surface of the water solution layer, they are completely or partially frozen. The partially frozen droplets are composed of the outer shells of the solidified tetradecane oil and central cores of the unsolidified oil as illustrated in Fig. 2. In this study, the oil droplet which has not started to solidify is referred to as an "oil droplet", the one which has started to solidify as a "frozen oil droplet" and as "partially frozen droplet". As illustrated in Fig. 1, the frozen oil droplets, which arrived at the surface of the water solution layer, were sampled and the amount of the frozen parts among them as the solidification fraction was measured by using a volumeter (10). Detail of measurement with the volumeter will be mentioned later. After the measurement of the solidification fraction, the melted tetradecane oil, removed from the volumeter, is returned to the oil tank. Some photographs were taken by using a camera (3) mounted above and near the side wall of the test section to observe the flow pattern and solidification characteristics of the dispersed phase droplets in the water solution layer.

Figure 2 shows a detail of the test section and nozzle used in this experiment. The test section is a vertical rectangle duct made of transparent acrylic resin plate of 10 mm in thickness and it has 100 mm square cross-section. The injection nozzle is fixed at the lower part of the test section. The vertical distance between the outlet of the nozzle and the top surface of water solution layer is fixed at 1.6 m $\pm$ 3 mm. Four thermocouples (T-type with 0.32 mm in diameter and with the measuring precision of $\pm 0.1$°C) are set in the test section, the two are set around the nozzle outlet and the others are in the upper part of the test section. All of the thermocouples used in this experiment were calibrated by a standard thermometer with the minimum temperature scale of 0.05°C and the measuring precision of temperature results in 0.1°C. Whole of the test section is covered with the Styrofoam thermal insulation with 50 mm thickness when visualization is not performed. As illustrated in Fig. 2, a nozzle is made of a fine stainless steel tube with a polyvinyl chloride (PVC) protector. It has dimensions of 1.0 mm in inner diameter, 2.0 mm in outer diameter and 64 mm in length. The inner diameter of the nozzle $d_n$ was decided with consideration of the dimension and freezing behavior of the oil droplet. The injecting oil temperature $T_n$ is measured by a thermocouple (T-type, 0.32 mm in diameter, the measuring precision is $\pm 0.1$°C) fixed at the bottom of the nozzle. Essentially, the injection temperature of tetradecane oil should be defined at the outlet of the nozzle. However, since little difference was observed between the temperatures of the tetradecane oil at the bottom of the nozzle and that at the outlet of it (within 0.1°C), the injection temperature of the tetradecane oil $T_n$ was obtained from the thermocouple fixed at the bottom of the nozzle.

The specific volume of tetradecane increases about

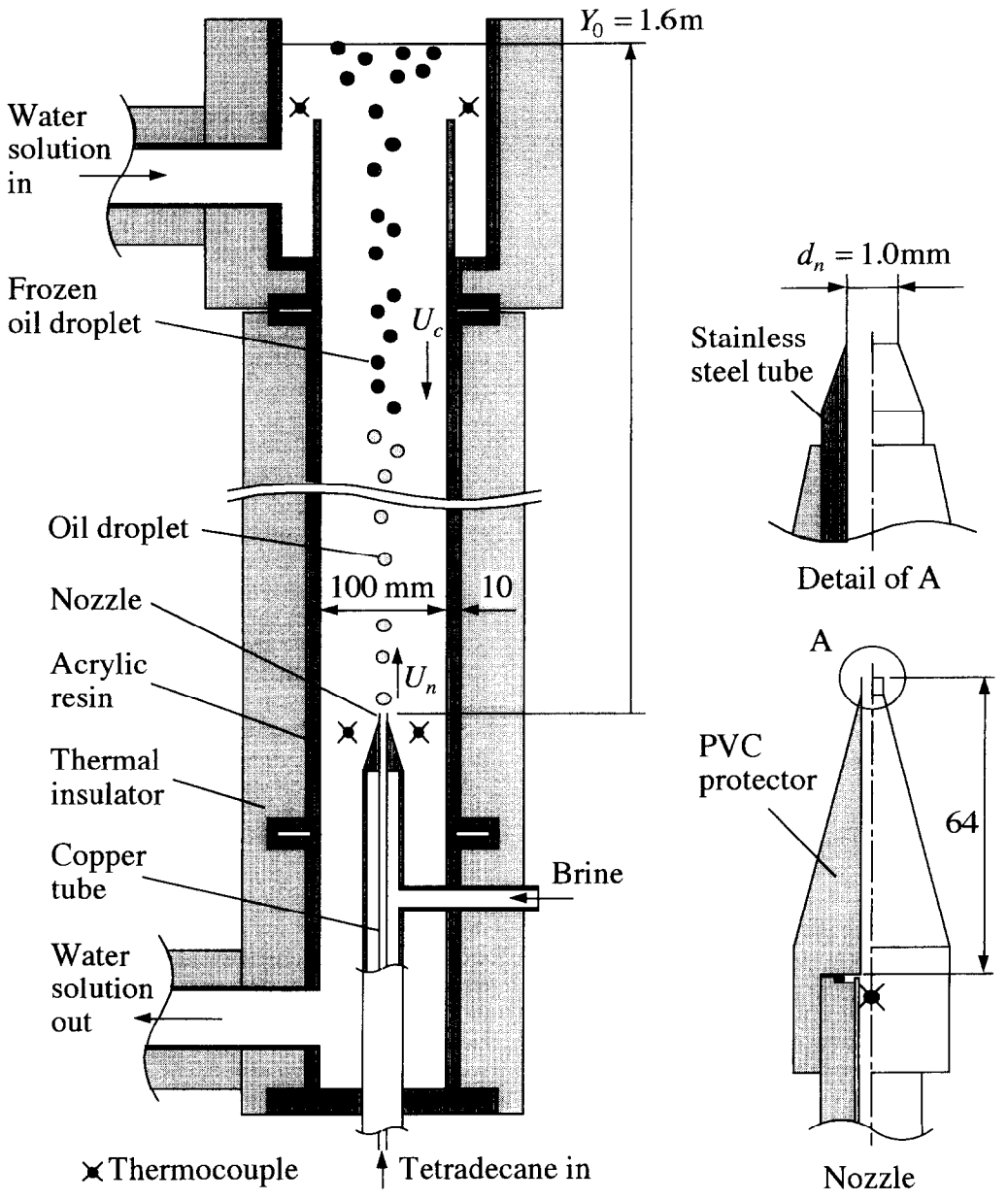


Fig. 2. Detail of test section and nozzle.

5.2% in a melting process. Therefore, the amount of frozen parts among the frozen oil droplets can be determined by measuring volume variation in the droplets by completely melting themselves. Figure 3 illustrates the volumeter which was used to measure the volume variation of the sampled frozen oil droplets. As shown in Fig. 3, it is constructed of a PVC airtight vessel with the inner volume of about 200 $cm^3$, the wire-mesh container of $40 \times 40 \times 20$ mm inside, and a glass tube with inner diameter of $5 \pm 0.02$ mm. A thermocouple (K-type, 0.32 mm in diameter, the measuring precision is 0.1°C) is inserted in the vessel to measure its inside temperature. The volume variation in the frozen oil droplets, packed in the vessel, can be measured as a displacement of a liquid level in a glass tube. The frozen oil droplets arrived at the water solution layer were successively transported to a water bath set at $5.8°C \pm 0.1°C$ (melting point of tetradecane) and were stored in the same temperature condition that they were sampled. The storing time of the droplets in the water bath is about 2 or 3 min. It was confirmed that there was no variation in the final quantity of the solidification with the storing time within 2 to 3 min. When enough sample droplets were accumulated in the water bath, they were packed in a wire-mesh container. Subsequently, the container is inserted into the volumeter containing a liquid phase tetradecane oil. The wire-mesh container and the volumeter and the liquid phase oil inside it are set at $5.8°C \pm 0.1°C$ beforehand by storing them in the water

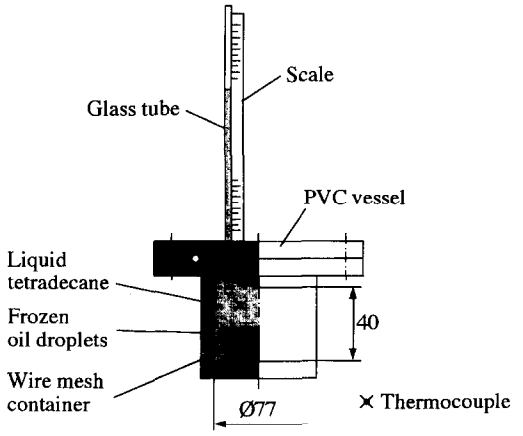


Fig. 3. Volumeter.

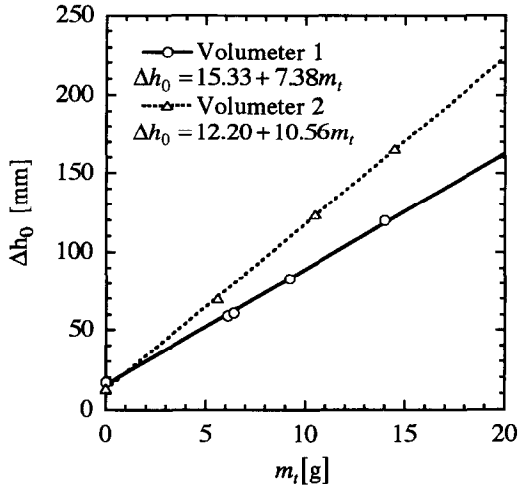


Fig. 4. Calibration results of the volumeter.

bath set at 5.8°C ± 0.1°C in order to prevent an extra phase-change in sampled oil droplets and then, the volumeter is immersed into the water bath set at 5.8°C and the liquid level in the glass tube $h_1$ is read, immediately. About 50–100 dispersed phase droplets were sampled in one run. The measurements were performed for 2 or 3 times in the same condition and an average of all runs were employed as a solidification rate. After measurement of $h_1$, the volumeter is heated to melt the sampled droplets inside it. When all the droplets were melted, the volumeter is transferred to another water bath set at 7.0°C ± 0.1°C and the liquid level in the glass tube $h_2$ is read when temperature of entire measuring device becomes constant. The volumeter itself expands or shrinks due to temperature variation. Hence, the measurements of $h_1$ and $h_2$ were performed under the same temperature conditions of 5.8°C and 7.0°C, respectively. The solidification fraction of the frozen oil droplets $R$ is defined as a mass fraction of solidified parts to the whole of the droplets. It is obtained by using the following equation

$$R = m_{tf}/m_t \times 100 = \Delta h/\Delta h_0 \times 100 \qquad (1)$$

where the parameter $m_{tf}$ is total mass of the solidified parts in all sampled droplets, $m_t$ is mass of whole of sampled droplets, $\Delta h$ is liquid level displacement in the glass tube measured at experiment ($= h_2 - h_1$) and $\Delta h_0$ is that when the solid phase tetradecane of mass $m_t$ is melted. The value of $\Delta h_0$ was obtained from a preliminary experiment. Figure 4 shows the correlations between $m_t$ and $\Delta h_0$. As shown in Fig. 4, the two volumeters were used in this experiment. The plotted marks in Fig. 4 represent the measured data and the lines show the calibration curves obtained by a least square fit for the obtained data. To check the measuring precision of this measuring device, some mixtures composed of liquid and solid phase tetradecanes with arbitrary mixing ratio were measured and the measuring precision was estimated within ±3.5%. In an actual experiment, the uncertainty of the entire measuring process of the solidification rate (from the sampling of the frozen oil droplets on the top surface of the water solution layer to the end of the measurement with the volumeter) is estimated to be within ±8.2%. It is seen that $\Delta h_0$ is proportional to $m_t$ on each device. The calibration lines and the measured data coincide within ±1.8.

## RESULTS AND DISCUSSION

*Flow and solidification characteristics of the dispersed phase droplets*

Figure 5(a) shows dispersion characteristics of tetradecane oil injected into the water solution, and solidification characteristics of oil droplets created by injection for three injection velocities; $U_n = 0.307$, 0.686 and 1.120 m/s. Tetradecane is transparent in a liquid phase and is white or opaque in a solid phase. Hence, photographs in Fig. 5(a) are taken by silhouetting the formed droplets against a sheet light source equipped behind the test section. In Fig. 5(a), transparent objects are oil droplets, and black ones are frozen oil droplets. From Fig. 5(a), it is seen that the tetradecane oil forms oil droplets and the droplets start to solidify during ascending and become the frozen oil droplets. It is observed that, with increasing $U_n$, the diameter of formed droplets reduces, and the number of droplets increases. It is noticed that there appears the difference of the height of water solution where the oil droplets start to solidify in the cases of $U_n = 0.686$ and 1.120 m/s in Fig. 5(a). It is considered that this variation occurs due to each distribution of droplet diameter, packing ratio and temperature of the water solution adjacent to the droplet and an existence of a super-cooling phenomenon in an oil droplet. As to the super-cooling phenomenon, however, since the water solution is repeatedly used, there exist some fine frozen oil droplets and impurities in the water solution layer (seen as fine black objects in the picture of Fig. 5(a)). Since these fine droplets and impurities act as nucleus for solidification, the oil droplets start to solidify with very small super-cooling

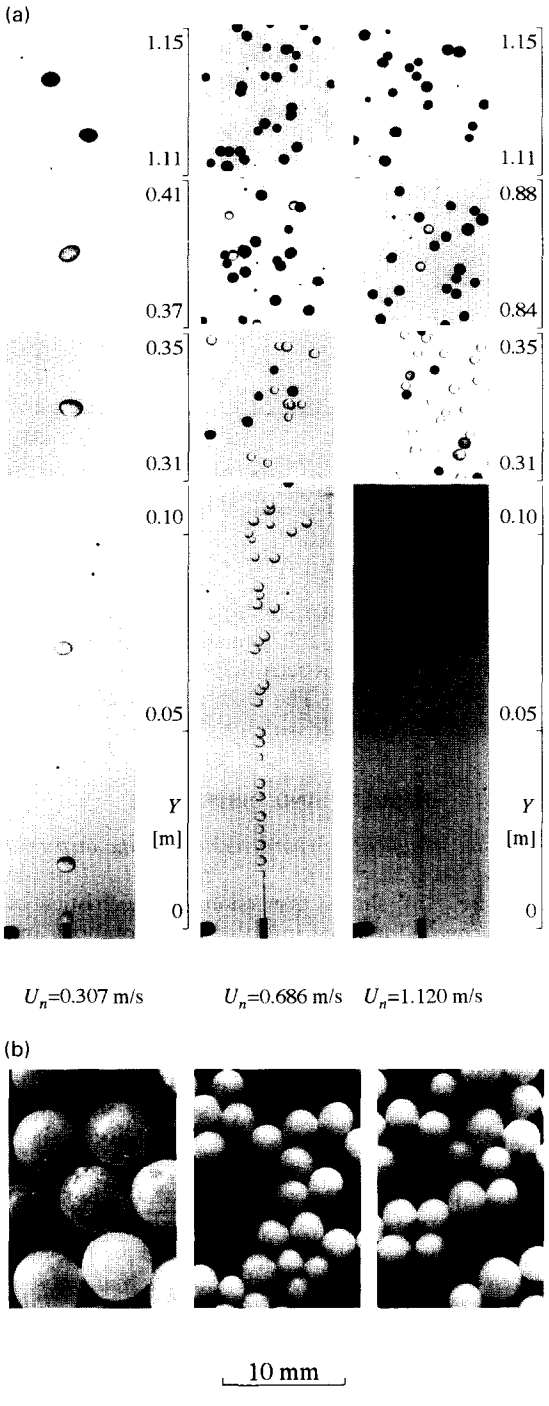


Fig. 5. Behavior of the formed droplets in the water solution ($T_n$ = 12°C, $T_c$ = 0°C): (a) dispersion and solidification characteristics of tetradecane oil droplets; (b) frozen oil droplets accumulated on the top surface of the water solution.

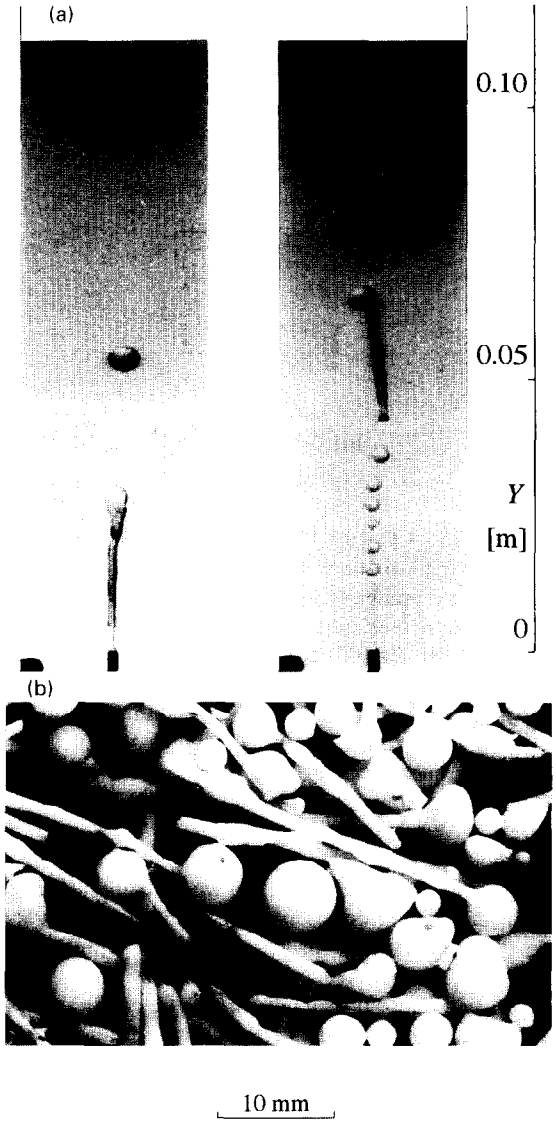


Fig. 6. Behavior of frozen oil column ($U_n$ = 0.686 m/s, $T_n$ = 19°C, $T_c$ = −3°C): (a) creation and breaking off of the frozen oil column; (b) frozen oil column and diameter-enlarged frozen oil droplets accumulated on the surface of the water solution.

degree in this experiment. Therefore, it was observed that all of the oil droplets start to solidify before they reach the surface of the water solution. A volumetric packing ratio of the formed droplets against the volume in which the droplets actually exist is less than 10% in the vicinity of an outlet of the nozzle and it is less than about 1% in the higher part of the test section. In this experiment, the volumetric packing ratio of the formed droplets is significantly low compared with that of the common spray tower [6]. Therefore, they can be treated as a single droplet. Figure 5(b) is a photograph of frozen oil droplets accumulated on the top surface of the water solution in the test section.

*Frozen oil column*

When injection temperature of tetradecane oil $T_n$ and/or the water solution temperature $T_c$ are relatively low, tetradecane oil freezes immediately at the outlet of the nozzle. Figure 6(a) shows a freezing of the

tetradecane oil near the outlet of the nozzle. As is seen in the figure, the frozen tetradecane oil forms a column-like shape. This object is referred to as the "frozen oil column" and the condition, that the frozen oil column is created, is referred to as the "frozen oil column formation condition", while, the condition that the frozen oil column is not created is referred to as the "normal injection condition". A frozen oil column repeats growing and breaking off from a nozzle as time elapses. The length and diameter of the column increase as it grows. In this condition, as seen in Fig. 6(a), the oil droplets are created from the tip hole of the frozen oil column and their diameters are enlarged, as compared with those in the normal injection condition. The frozen oil column is composed of the tube-like solidified outer shell and liquid phase oil flowing inside it. The frozen oil column leaves from the nozzle and ascends in the water solution with the liquid phase oil inside it. Figure 6(b) shows the frozen oil column and diameter-enlarged oil droplets accumulated on the top surface of the water solution.

*Mean diameter of the formed droplet*

Figure 7 indicates the relationship between an arithmetic mean diameter of the formed droplets $\bar{d}_p$ and an injection velocity of tetradecane oil $U_n$, when the normal injection is performed. The value of $\bar{d}_p$ was determined by measuring the size of the droplets on the photographs by using a vernier calliper. Since the shape of frozen oil droplets is changed from a sphere to an ellipsoid when the size of them is relatively large, the diameter of the frozen oil droplet was determined as the diameter of an equivalent sphere which has the same volume as that of the real droplet. The volume of a formed droplet was determined by regarding it as a spheroid. The tetradecane droplet shrinks about 1.7% in diameter by solidification. Therefore, the diameter variation in the dispersed phase droplet can be neglected in the present study. As indicated in the

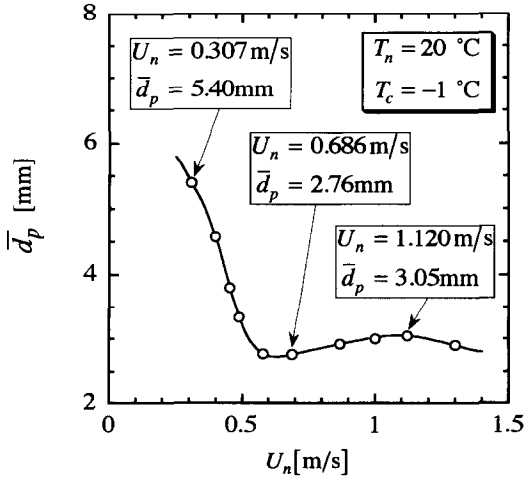


Fig. 7. Mean droplet diameter of the formed droplets $\bar{d}_p$ vs injection velocity of tetradecane oil $U_n$.

Table 2. Mean droplet diameters for each injection oil velocity

| $U_n$ [m/s] | $\bar{d}_p$ [mm] |
|---|---|
| 0.307 | 5.40 |
| 0.686 | 2.76 |
| 1.120 | 3.05 |

figure, the value of $\bar{d}_p$ reduces sharply and becomes a minimum with increasing $U_n$. Then it slightly increases and becomes maximum and decreases again with an increase in $U_n$. The uncertainty in the measuring results of $\bar{d}_p$ is within $\pm 1.5\%$. The solidification experiments were performed for three injection velocities of $U_n$ = 0.307, 0.686 and 1.120 m/s, as indicated in the figure. The values of $\bar{d}_p$ under each condition of $U_n$ are indicated in Table 2.

*Solidification fraction of the oil droplets*

Figures 8(a)–(c) show the relationship between the solidification fraction $R$ of the frozen oil droplets and injection temperature of tetradecane oil $T_n$ for three injection velocity $U_n$ = 0.307, 0.686 and 1.120 m/s, respectively. The oil droplets were sampled on the surface of the water solution. The solid lines in the figures show the results under the normal injection condition and the dotted lines under the frozen oil column formation condition. As shown in the figures, the value of $R$ increases with a decrease in $T_n$ under the normal injection condition (solid lines) and $R$ decreases with a decrease in $T_n$ in the frozen oil column formation condition (dotted lines). $R$ becomes maximum at the boundary injection temperature of tetradecane oil between normal injection condition and the frozen oil column formation one. In the normal injection condition, a decrease in $T_n$ leads to a reduction of sensible heat of the oil droplet, therefore, the starting position of solidification of the oil droplet shifts to the lower one in the test section. As a result, the value of $R$ increases since the ascending duration of the frozen oil droplet increases. In the frozen oil column formation condition, a decrease in $T_n$ makes the frozen oil column larger. The sizes of the frozen oil column formed from the nozzle and of the oil droplet created from the tip hole of the column are enlarged, as the $T_n$ decreases. Since the frozen oil column contains a liquid phase oil inside it, the column takes longer time to freeze completely as it becomes larger. The thermal resistance of the solidified part in the column increases with an increase in the column size. Therefore, the solidification fraction of the frozen oil column decreases with a decrease in $T_n$.

Referring to $T_c$, as shown in Fig. 8, the value of $R$ increases with a decrease in $T_c$ since the decrease in $T_c$ promotes the freezing of the frozen oil droplets and frozen oil column. However, the thermal resistance of the solidified part in the frozen oil droplet increases with an increase in $R$. Therefore, it is seen that the

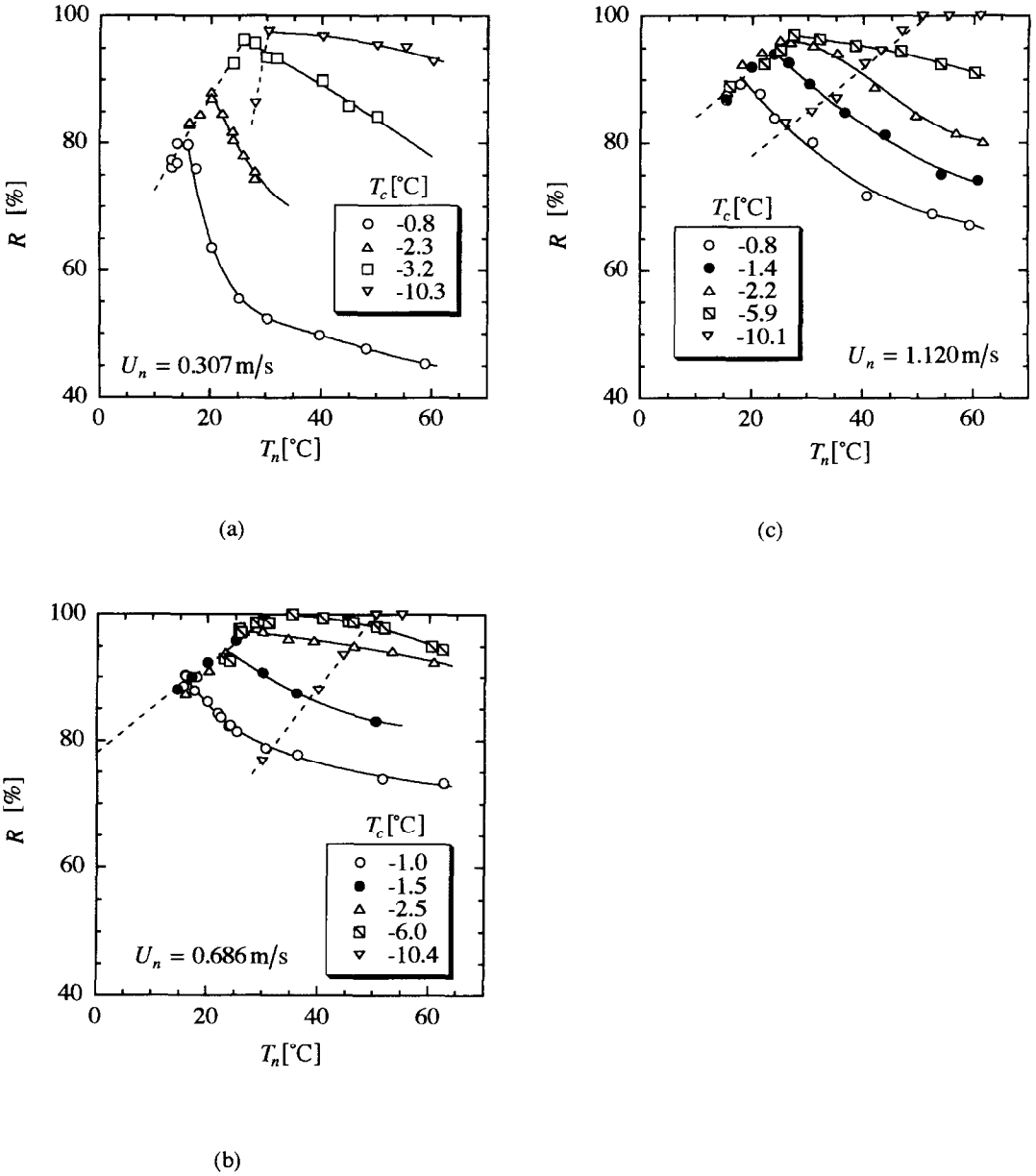


Fig. 8. Solidification fraction $R$ for injecting tetradecane oil temperature $T_n$: (a) $U_n = 0.307$ m/s; (b) $U_n = 0.686$ m/s; (c) $U_n = 1.120$ m/s.

increasing rate of $R$ against $T_c$ becomes smaller as $T_c$ decreases. However, it is understood that the $R$ decreases with a decrease in $T_c$ in the frozen oil column formation condition at lower temperatures of $T_c$ ($T_c = -3.2 \sim 10.3$°C in Fig. 8(a), $T_c = -6.0 \sim -10.4$°C in Fig. 8(b) and $T_c = -5.9 \sim -10.1$°C in Fig. 8(c)). In this condition, a decrease in $T_c$ makes the frozen oil column and droplet larger considerably, therefore, it is difficult for them to freeze completely due to the high thermal resistance of solidified layer. As a result, the $R$ decreases with a decrease in $T_c$ under the frozen oil column formation condition for lower $T_c$.

From Fig. 8(a)–(c), it is noticed that the value of $R$ at $U_n = 0.307$ m/s (Fig. 8(a)) is the lowest, the $R$ at $U_n = 1.120$ m/s (Fig. 8(c)) is the second and $R$ at $U_n = 0.686$ m/s (Fig. 8(b)) is the highest, as comparing them in the same ranges of $T_n$ and $T_c$. These variations occur due to the difference in the droplet diameter at each condition of $U_n$ as indicated in Table 2. It is understood that the solidification fraction increases with a decrease in droplet diameter. It is difficult for an oil droplet to freeze completely as the diameter increases. Furthermore, the ascending velocities of the oil droplet and the frozen oil droplet increase with an increase in the droplet diameter. Therefore, an increase in the droplet diameter causes a reduction in an ascending period, which results in the reduction of

the solidification fraction. An increase in an ascending velocity also leads an increase in heat transfer coefficient on the surface of the droplet, however, it has less effect on solidification due to a reduction of an ascending period of the droplet.

*Non-dimensional data reduction of the solidification fraction*

The data reduction of the solidification fraction was performed. The relating experimental parameters are the injection oil temperature $T_n$, water solution temperature $T_c$ and ascending velocity of the dispersed phase oil droplets. In this study, the $T_n$ is expressed as nondimensional temperature ratio $\theta$ defined as follows:

$$\theta = (T_n - T_m)/(T_m - T_c). \tag{2}$$

The numerator of the equation (2) expresses the sensible heat variation of the oil droplet between the injection and the beginning of the solidification. The denominator of the equation (2) means the cooling capacity of the water solution against the oil droplet. Therefore, equation (2) expresses the relative cooling ratio of the water solution to the oil droplet before a solidification. The water solution temperature $T_c$ is expressed as Stefan number *Ste* defined as follows:

$$Ste = c_{ds}(T_m - T_c)/L \tag{3}$$

where $c_{ds}$ is the specific heat of solid phase tetradecane and $L$ is the latent heat of tetradecane. This parameter expresses the relative cooling capacity of the water solution to proceed the solidification of a frozen oil droplet. The characteristics of the ascending velocity are mentioned in the next section.

*Ascending velocity of the formed droplets*

Figure 9(a)–(c) show the relationship between the absolute velocity of the formed droplet $U_p$ and the vertical location $Y$ for three injection oil velocity; $U_n = 0.307$, 0.686 and 1.120 m/s, respectively. The $U_p$ is given by following equation:

$$U_p = V_d/(\varepsilon \cdot F) \tag{4}$$

where $V_d$ is volumetric flow rate of tetradecane oil and $F$ is the sectional area of the group of ascending the formed droplets. In equation (4), the $\varepsilon$ is the local packing ratio of the formed droplets defined as following expression:

$$\varepsilon = N \cdot (4/3)\pi(\bar{d}_p/2)^2/(F \cdot \Delta Y) \tag{5}$$

where $F \cdot \Delta Y$ is a quantity of the test volume at height $Y$ and $N$ is the number of formed droplets included in the test volume $F \cdot \Delta Y$. $N$ was obtained by a visual observation by using a video camera. The uncertainty in $U_p$ associated with the visual observation is estimated to be within $\pm 3\%$. In Figs. 9(a)–(c), the value of $U_p$ at $Y = 0$ means the injection velocity of oil $U_n$ at the nozzle outlet. As seen in the figures, the value of $U_p$ reduces sharply after that the droplet leaves from the outlet of the nozzle, and approaches to the terminal velocity of the oil droplet. Then the oil droplet freezes and its outer surface changes to a solid phase. Therefore, it behaves such like a rigid sphere. A rigid sphere has a higher drag coefficient as compared with a liquid droplet, therefore, the value of $U_p$ decreases sharply again and approaches to the terminal velocity of the frozen oil droplet.

It is convenient to define the characteristic ascending velocity of the formed droplet in order to define the non-dimensional parameter which expresses the droplet motion during the ascending. In this study, as indicated in Fig. 9(a)–(c), the ascending velocity at the starting position of solidification $U_{pc}$, which is graphically decided in the figures, was used as the characteristic velocity. Then, the non-dimensional parameter which expresses the ascending velocity of the dispersed phase droplet is defined as Reynolds number $Re_{pc}$ as follows:

$$Re_{pc} = (U_{pc} - U_c) \cdot \bar{d}_p/\nu_c \tag{6}$$

*Nondimensional data reduction of the solidification fraction*

Figure 10(a) and (b) represent the relationship between the modified solidification fraction $R^*$ and the modified temperature ratio $x$. As mentioned in Fig. 8(a)–(c), the dependency of $R$ on the water solution temperature $T_c$ is different in the range of $T_c$. Therefore, the *Ste* number, which includes $T_c$, is classified into two ranges indicated in Fig. 10(a) and (b). In Fig. 10(a) and (b), the $R^*$ is determined by generalizing $R$ in dependency of the maximum $R$ value in each condition (see Fig. 8(a)–(c)) on *Ste* and $Re_{pc}$. The $x$ is determined by generalizing $\theta$ in dependency of $\theta$ at the maximum $R$ value on *Ste* and $Re_{pc}$. Since the maximum $R$ value in the condition of Fig. 10(b) is almost constant for *Ste*, the ordinate in this figure does not contain the *Ste*. As shown in the figures, there is a maximum $R^*$ on the distribution of the data, which represent the maximum value of $R$. The left side region of the maximum $R^*$ corresponds to the frozen oil column formation condition and the right side region corresponds to the normal injection condition.

The empirical equations of the solidification fraction for each condition are also drawn in the figures (equations (7)–(10)), which are derived by the least square method to each data group. The equations (7)–(10) and the applicable range of them and the relative errors between the measured data and the equations are summarized in Table 3. Equations (7)–(10) are arranged for $R$ and they are derived in terms of *Ste*, $Re_{pc}$ and $\theta$. The boundary conditions of the applicable range for equations (7) and (8) and of equations (9) and (10) are determined as the intersections of equations (7) and (8) and of equations (9) and (10), respectively. These intersections also correspond to the conditions that show the maximum value of $R$. The *Ste* has the positive exponent in the empirical equations

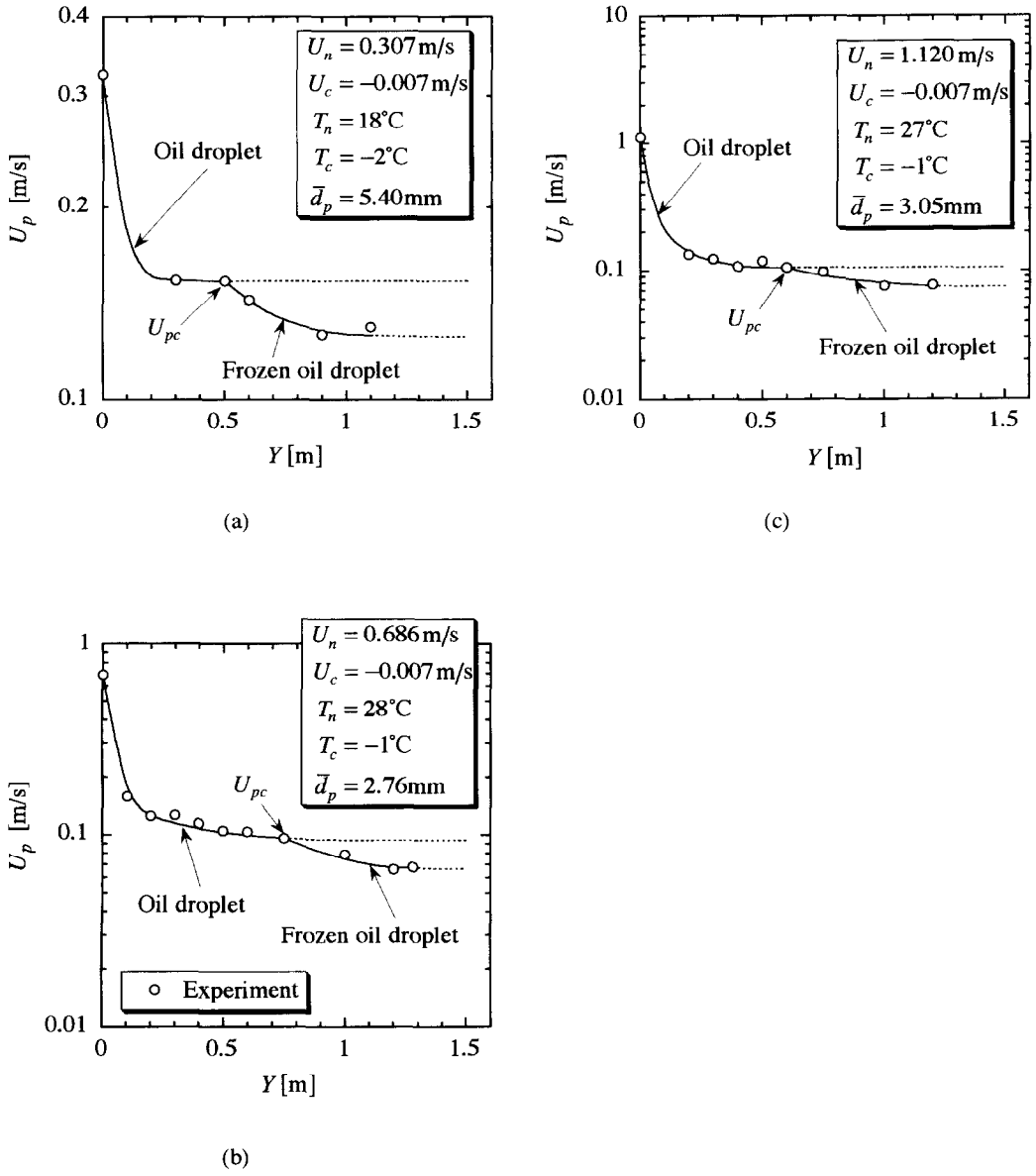


Fig. 9. Variation of ascending velocity of the formed droplets $U_p$ for the drop height $Y$: (a) $U_n = 0.307$ m/s; (b) $U_n = 0.686$ m/s; (c) $U_n = 1.120$ m/s.

for the lower *Ste* condition in equations (7) and (8) and in the normal injection condition for higher *Ste* condition in equation (10). This positive exponent represents that the $R$ increases with an increase in *Ste* (which means the reduction in $T_c$) in the lower *Ste* condition due to the increase of cooling capacity of the water solution. On the other hand, the *Ste* has a negative exponent in the equation (9) for the frozen oil

Table 3. Empirical equations of solidification rate of frozen oil droplets

| Condition | | Equation | Equation no. | Deviation |
|---|---|---|---|---|
| $0.043 < Ste < 0.081$ | | | | |
| Frozen oil column formed | $\theta/(Ste^{0.938} \cdot Re_{pc}^{-0.370}) < 164$ | $R = 413 Ste^{0.475} \cdot Re_{pc}^{0.0547} \cdot \theta^{0.102}$ | (7) | ±6.2% |
| Normal injection | $164 \leqslant \theta/(Ste^{0.938} \cdot Re_{pc}^{-0.370})$ | $R = 1880 Ste^{0.754} \cdot Re_{pc}^{-0.165} \cdot \theta^{0.195}$ | (8) | ±7.3% |
| $0.081 \leqslant Ste < 0.13$ | | | | |
| Frozen oil column formed | $\theta/(Ste^{0.602} \cdot Re_{pc}^{-0.135}) < 17.5$ | $R = 83.7 Ste^{-0.0960} \cdot Re_{pc}^{0.0484} \cdot \theta^{0.160}$ | (9) | ±7.3% |
| Normal injection | $17.5 \leqslant \theta/(Ste^{0.602} \cdot Re_{pc}^{-0.135})$ | $R = 187 Ste^{0.0720} \cdot Re_{pc}^{0.0862} \cdot \theta^{-0.120}$ | (10) | ±3.1% |

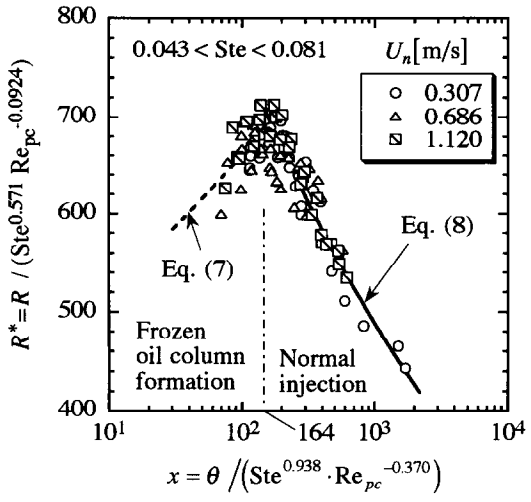


(a)

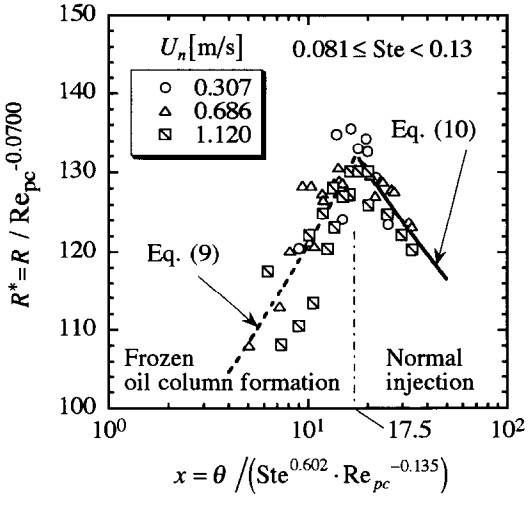


(b)

Fig. 10. Modified solidification fraction $R^*$ of the frozen oil droplets versus modified temperature ratio $x$: (a) $0.043 < Ste < 0.081$; (b) $0.081 \leqslant Ste < 0.13$.

column formation condition in higher *Ste* condition, since the $R$ decreases with increasing of *Ste* due to the enlargement of the frozen oil column. The $\theta$ has the negative exponent in the empirical equations for the normal injection condition in equations (8) and (10), and it has the positive exponent in equations (7) and (9) for the frozen oil column formation condition. The $\theta$ represents $T_n$ indirectly, therefore the $R$ increases with a decrease in $\theta$ in the normal injection condition due to the reduction of a sensible heat of an oil droplet and the $R$ decreases with a decrease in $T_n$ in the frozen oil column formation condition due to the enlargement of the frozen oil column and droplet. The $Re_{pc}$ has the negative exponent in all equations of equations (7)–(10). The increase in $Re_{pc}$ means an increase of ascending velocity of the droplet. As a result, the heat transfer coefficient between droplet and water solution increases. However, the ascending duration of the droplet in the water solution decreases. Since the ascending duration of the droplet in the water solution layer has a higher influence on the amount of total transferred heat, the increase in ascending velocity ($Re_{pc}$) causes a reduction in the solidification fraction $R$. The uncertainty in the value of $R$ is estimated to be within $\pm 8.2\%$. The uncertainties in $\theta$ and *Ste* associated with the temperature measurement are estimated to be within $\pm 2.2$ and $\pm 1.5\%$, respectively. The uncertainty in $Re_{pc}$ due to the measuring errors of $U_{pc}$ and $\bar{d}_p$ is within $\pm 4.5\%$. Hence, the uncertainty in the value of applicable range-boundary of equations (7)–(10) in Table 3 is estimated to be in the range of $\pm 3.1$–$\pm 7.3\%$.

## CONCLUSION

The study of the solidification characteristics of the oil droplet ascending in a low temperature water solution layer was performed. The results obtained in this research are summarized as follows.

The solidification fraction of the frozen oil droplets $R$ is expressed as functions of *Stefan number Ste*, droplet Reynolds number $Re_{pc}$ and nondimensional temperature ratio $\theta$. They have different characteristics in the condition of $0.043 < Ste < 0.081$ and $0.081 \leqslant Ste < 0.13$ and in the normal injection condition and frozen oil column formation one. The optimum operating condition in which the maximum $R$ value can be obtained, is given as the boundary point between the normal injection condition and the frozen oil column formation one. At any condition, the value of $R$ decreases with an increase in the droplet Reynolds number $Re_{dc}$ since a decrease in ascending duration of the formed droplets in the water solution layer overcomes the effect of the heat transfer coefficient between the droplets and the water solution on promotion of oil droplet solidification.

*Acknowledgement*—The authors would like to express their thanks to Mr Yasuhiro Yoshida and Mr Sou Tadatomo for aid in the present experiment.

## REFERENCES

1. Yamada, M., Fukusako, S. and Horibe, A., Direct-contact heat-transfer characteristics from a liquid ice layer. *Experimental Heat Transfer: Fluid Mechanics and Thermodynamics*, 1993, 1682–1687.
2. Inaba, H. and Morita, S., Thermophysical properties of low temperature latent heat emulsion. *Proceedings of the 14th Symposium on Thermophysical Properties*, 1993, pp. 307–310.
3. Keith, F. W. and Hixon, A. N., Liquid–liquid extraction spray columns: drop formation and interfacial transfer area. *Industrial Engineering Chemistry*, 1955, **47**(2), 258–267.
4. Letan, R. and Kehat, E., The mechanics of heat transfer in a spray column heat exchanger. *A.I.Ch.E. Journal*, 1970, **16**(6), 955–963.
5. Moresco, L. L. and Marschall, E., Liquid–liquid direct-

contact heat transfer in a spray column. *ASME Journal of Heat Transfer*, 1980, **102,** 684–687.
6. Jacobs, H. R., Direct-contact heat transfer for process technologies. *ASME Journal of Heat Transfer*, 1988, **110,** 1259–1270.
7. Hayworth, C. B. and Treybal, R. E., Drop formation in two-liquid-phase systems. *Industrial and Engineering Chemistry*, 1950, **42**(6), 1174–1181.
8. Tanasawa, T. and Toyoda, S., On the atomization of liquid jet issuing from a cylindrical nozzle. Technical Report of Tohoku University, Vol. 19-2, 1955, pp. 135–156.
9. Scheele, G. F. and Meister, B. J., Drop formation at low velocities in liquid–liquid systems. *A.I.Ch.E. Journal*, 1968, **14**(1), 9–19.
10. Hu, S. and Kintner, R. C., The fall of single liquid drops through water. *A.I.Ch.E. Journal*, 1955, **1**(1), 42–48.
11. Licht, W. and Narasimhamurty, G. S. R., Rate of fall of single liquid droplets. *A.I.Ch.E. Journal*, 1955, **1**(3), 366–373.
12. Sideman, S. and Taitel, Y., Direct-contact heat transfer with change of phase : evaporation of drops in an immiscible liquid medium. *International Journal of Heat and Mass Transfer*, 1964, **7,** 1273–1289.
13. Sideman, S. and Hirsch, G., Direct-contact heat transfer with change of phase : condensation of single vapor bubbles in an immiscible liquid medium : preliminary studies. *A.I.Ch.E. Journal*, 1965, **11**(6), 1019–1025.
14. Fujita, Y., Hirahaya, K., Matsuo, S. and Nishikawa, K., Heat transfer characteristics in direct contact evaporation process. *Proceedings of the 2nd ASME/JSME Thermal Engineering Joint Conference*, Vol. 4, 1987, pp. 119–126.
15. Umano, S., Direct-contact refrigeration. *Japanese Government Chemical Industry Research Publication*, 1959.
16. Mehrabian, R., Kear, B. H. and Coheu, M., *Rapid Solidification Processing*. Clasitor's Pub., 1978.
17. Siegel, R., Analysis of solidification interface shape during continuous casting of a slab. *International Journal of Heat and Mass Transfer*, 1978, **21,** 1421–1430.
18. Fetecau, C. and Petrescu, S., Heat transfer at spherical thin film solidification. *Acta Mechanica*, 1992, **91,** 107–111.
19. Petrescu, S., Transferul de caldura la cristalizarea din topitura. *Revista de Chimie*, 1992, **1**(2), 44–49.
20. Petrescu, S. and Fetecau, C., Liquid–liquid heat transfer at direct contact : accompanied by solidification : the cooling stage. *Acta Mechanica*, 1993, **99,** 213–218.
21. Filipescu, L., Proprietatile fizico-mecanice ale ingrasamintelor granulate, Bucuresti, Editura M.I.Ch., 1987.
22. Onu, P., Ginju, D. and Luca, C., Granularea zeolitilor. *Lucrarile Sesiunii Jubiliare de Comunicari Stiintifice*, 1988, **10,** 46–49.
23. Inaba, H. and Sato, K., Fundamental study on latent cold heat storage by means of oil droplets with low freezing point : 1st report : flow and solidification characteristics of tetradecane droplets ascending in low-temperature water solution. *Transactions of JSME Series B*, 1994, **60**(580), 4236–4243.
24. Inaba, H. and Sato, K., Fundamental study on latent cold heat storage by means of oil droplets with low freezing point : 2nd report : nondimensional analysis of solidification and heat transfer characteristics of tetradecane oil droplets ascending in low-temperature water solution. *Transactions of JSME Series B*, 1996, **62**(593), 325–332.